An integrated drug repurposing strategy for the rapid identification of potential SARS-CoV-2 viral inhibitors

Trezza Alfonso[1#], Iovinelli Daniele[1#], Prischi Filippo[2*], Santucci Annalisa[1] and Spiga Ottavia[1*]

[1] Department of Biotechnology, Chemistry and Pharmacy, University of Siena, 53100, Siena, Italy
[2] School of Life Sciences, University of Essex, Colchester, CO4 3SQ, UK

alfonso.trezza2@unisi.it,
daniele.iovinelli@student.unisi.it
fprischi@essex.ac.uk
annalisa.santucci@unisi.it
ottavia.spiga@unisi.it

[#]contributed equally
[*]corresponding authors: ottavia.spiga@unisi.it; fprischi@essex.ac.uk

Abstract

The Coronavirus disease 2019 (COVID-19) is an infectious disease caused by the severe acute respiratory syndrome–coronavirus 2 (SARS-CoV-2). The virus has rapidly spread in humans, causing the ongoing Coronavirus pandemic. Recent studies have shown that, similarly to SARS-CoV, SARS-CoV-2 utilises the Spike glycoprotein on the envelope to recognise and bind the human receptor ACE2. This event initiates the fusion of viral and host cell membranes and then the viral entry into the host cell. Despite several ongoing clinical studies, there are currently no approved vaccines or drugs that specifically target SARS-CoV-2. Until an effective vaccine is available, repurposing FDA approved drugs could significantly shorten the time and reduce the cost compared to de novo drug discovery. In this study we attempted to overcome the limitation of in silico virtual screening by applying a robust *in silico* drug repurposing strategy. We combined and integrated docking simulations, with molecular dynamics (MD), Supervised MD (SuMD) and Steered MD (SMD) simulations to identify a Spike protein – ACE2 interaction inhibitor. Our data showed that Nilotinib and Imatinib bind the receptor-binding domain of the Spike protein with high affinity and prevent ACE2 interaction.

Introduction

The World Health Organisation (WHO) declared the Coronavirus disease (COVID-19) outbreak as pandemic on the 12 of March 2020, and as of April 16, about two million cases and nearly 130,885 deaths have been reported *(https://www.who.int/emergencies/diseases/novel-coronavirus-2019/situation-reports/)*. The Severe acute respiratory syndrome–coronavirus 2 (SARS-CoV-2) was identified as the viral agent causing the disease. SARS-CoV-2 is closely related to the SARS-CoV, which caused a pandemic in 2002-2003 [1,2], and it is believed to be the third member of the *Coronaviridae* family to cause severe respiratory diseases in human [3,4]. Despite several ongoing clinical studies, there are currently no approved vaccines or drugs that specifically target SARS-CoV-2.

SARS-CoV-2 has a single-stranded positive-sense RNA composed of 29,903 nt containing five genes, *ORF1ab* (codifying 16 non-structural proteins), *spike* (S), *envelope* (E), *membrane* (M) and *nucleocapsid* (N) genes [5] The virus uses the S homotrimeric glycoprotein located on the virion surface to allow entry into the human cells [6] The S protein goes through major structural rearrangements to mediate viral and human cell membranes fusion. The process is initiated by the binding of the receptor-binding domain (RBD) of the S1 subunit to the peptidase domain (PD) of angiotensin-converting enzyme 2 receptor (ACE2) on the host cell [7]. Structural studies have shown that two S protein trimers can simultaneously bind to one ACE2 dimer [8]. This induces a conformational change that expose a proteolytic site on the S protein, which is cleaved by the cellular serine protease TMPRSS2 [9]. Dissociation of S1 induces transition of the S2 subunit to a postfusion conformation, with exposed fusion peptides [10], which allows endocytic entry of virus [11]. Wrapp et al. [12] have shown that, despite SARS-CoV-2 and SARS-CoV share a similar cell entry mechanism, SARS-CoV-2 S protein binds ACE2 with a 10- to 20-fold higher affinity than SARS-CoV S, which may be related to the higher person-to-person transmission of SARS-CoV-2.

S glycoprotein is highly immunogenic, and it is a promising target for drug design (Bongini et al., 2020). Indeed, we showed that a combination of four 20-mer synthetic peptides disrupting SARS-CoV S heterotrimer reduced or completely inhibited infectivity *in vitro* [13]. Similarly, antibodies targeting SARS-CoV S protein neutralize the virus and have potential for therapy [14]. In fact, disruption of the binding of the S protein to ACE2 prevents the virus from attaching to the host cell [15]. The social and economic impact of COVID-19 and the possibility of future similar pandemics is pushing for a rapid development of treatments. As such, targeting viral-host protein-protein interaction (PPI) may represent a promising way to prevent or reduce the spreading of the virus before a vaccine is available [16]. In this study, we performed an extensive analysis of the intrinsic dynamic, structural properties and drug targeting of SARS-CoV-2 RDB. In particular starting from the structure of RDB in complex with ACE2, we identified transient pockets on RDB on the ACE2 interaction surface area. Our data provide detailed information on the dynamic features of RDB

that we exploited for docking studies. We carried out a virtual screening using 1223 FDA-approved drugs to explore new therapeutic benefits of existing drugs. To take into account molecules unique features, such as conformational flexibility, charges distribution, and solvent role in target recognition and binding, we implemented an extensive molecular dynamics simulation analysis. By combining molecular dynamics simulations (MD), Supervised MD (SuMD), Steered MD (SMD) and free energy calculations, we showed that Nilotinib and Imatinib bind RDB with high affinity and prevent ACE2 interaction. Overall, by adopting a robust in silico approach, our results could open the gates toward the development of novel COVID-19 treatments.

Results

SARS-CoV-2 S glycoprotein virtual screening

SARS-CoV-2 RBD and hACE2 binding is mostly driven by polar interaction, with an overall ~900Å^2 buried surface area. A close analysis of the interface reveals the absence of cavities on RBD in the interaction surface. We performed MD simulations to account for the protein conformational flexibility and detected 1029 transient pockets. Based on the druggability features of the cavities, i.e. volume, depth, polarity, and proximity to the hACE2 binding site, we detected a cluster of 9 transient pockets. In order to identify possible PPI inhibitors, the transient pocket that contained key residues involved in hACE2 recognition and binding (Fig. 1.A) was selected and used for the virtual screening of 1223 FDA-approved drugs. Best 10 compounds showed high binding free energy scores (8.3 to -7.1 Kcal/mol) (Fig. S1). The compounds with the highest binding energies were Nilotinib and Imatinib, two related aminopyrimidine-based ATP competitive BCR–ABL1 inhibitors used for the treatment of chronic myeloid leukaemia [17]. These two compounds share a similar structure and bind RBD in a similar way, with the aminopyrimidine ring forming H-bonds with Asp405, Gln409 and hydrophobic interaction with Val417 and Leu455, the central amide group forming H-bonds with Lys403 and Tyr453, and the benzamide ring forming π-stacking with Tyr505 (Fig. 1.B-C) The higher binding score of Nilotinib is linked to the presence of two extra H-bonds with Gln414 and Asn501. Importantly, these are biologically relevant residues, since Asp403, Val417, Leu455 are located at the RBD-ACE2 interface, and Tyr453, Asn501 and Tyr505 form H-bonds with ACE2. Taken together, these data show that Nilotinib and Imatinib are able to form clearly defined specific interaction with the SARS-CoV-2 S glycoprotein.

Nilotinib and Imatinib inhibit RBD-ACE2 binding *in silico*

In order to understand if Nilotinib and Imatinib are able to interfere and prevent the binding between the S glycoprotein and ACE2, we run a Supervised Molecular Dynamics (SuMD)

simulations. Using SuMD it is possible to simulate the full binding process of ACE2 to RBD in presence of Nilotinib or Imatinib in an unbiased way (i.e. independently from starting relative position), taking into account hydration patterns and drug binding-unbinding events. We first validated the SuMD protocol by simulating the binding process of RBD with ACE2. The resulting relative position of ACE2 bound to RBD is comparable to that in the crystal structure (Fig. S2). The interaction between ACE2 and RBD is established after 2 ns of productive trajectory and is mediated by key residues in the receptor binding motif (RBM). Specifically, Phe486, Asn487, Tyr489 in the loop in the ACE2-binding ridge, and Tyr449, Tyr453, Leu455, Phe456, Gln493, Gln498, Asn501 and Tyr505. Using the same approach, we then simulated the binding of ACE2 to RBD bound to Nilotinib or Imatinib. During the SuMD simulation ACE2 did not displace the drugs and did not form interactions with the S glycoprotein even after 50 ns of simulation. This is very likely due to the drugs interacting with the key residues Leu455, Gln493, and Tyr505, which prevent ACE2 target recognition. Taken together these data show that Nilotinib and Imatinib prevent ACE2 recognition and binding to the S glycoprotein.

Nilotinib and Imatinib binding stability

During the SuMD drugs were allowed to move and find a more energetically favourable pose in the binding pocket. However, we noticed that Nilotinib and Imatinib moved in different ways, and, in order to investigate this further, we performed 100 ns cMD simulations of RBD alone and in complex with the drugs. While the pose of Nilotinib did not change much during the simulation, Imatinib moved significantly (Fig. S3.A-B). This is linked to the presence of the trifluoromethyl group on Nilotinib which allows the drug to form halogen bonds, specifically with Gln493 in the optimised pose. In order to exclude presence of artefacts in our analysis, we monitored the protein structural integrity during the simulations. We noticed limited differences between the RMSD of the apo protein and the RMSD of RBD-Nilotinib/Imatinib complexes, which excludes presence different protein structural rearrangements in the three cMD simulations (Fig. S3.C). We then estimated the average binding free energy for the two compounds, and the contribution of each RBD residue to the binding energy during a 10 ns MD simulation. The affinities estimated by the MM/PBSA calculations show that ligands bind spontaneously to the target and with high affinity, -286 KJ/mol and -296 KJ/mol for Nilotinib and Imatinib respectively (Fig. 2.A). Per residue binding energy contribution showed that Val417, Leu455 and Tyr489 were the key binding residues for Imatinib, while Phe456, Phe486 and Tyr489 were the key binding residues for Nilotinib. Importantly, we noticed that Arg355, Lys378, Lys403, Arg408, Asp420, Asn422, Lys452 showed, although low in magnitude, positive values of binding energy for Imatinib, but not for Nilotinib, suggesting a less favourable interaction of RBD with Imatinib (Fig 2.B). Taken together these data suggest that Nilotinib and Imatinib have differences in binding modes.

Drugs-protein unbinding simulations

To further characterise the recognition process of the two drugs to the S glycoprotein we performed Steered Molecular Dynamics (SMD) simulations. We ran a 500 ps SMD simulation on RBD in complex with both Nilotinib and Imatinib, and the time-averaged force profiles during the unbinding simulation of complexes is shown in Fig. 3.A. For Nilotinib a steady increase of the applied forces can be seen on the first ~150 ps of the simulation, until it reaches the maximum, which corresponds to the rupture force of Nilotinib unbinding along this dissociation pathway. The force then quickly decreases and stays constant till the end of the simulation. Presence of multiple peaks suggests a 3-steps unbinding process. In the first step (0-172ps) Nilotinib moves away from the transient pocket sliding along the flexible loop in the ACE2-binding ridge, in the second step (173-194 ps) Nilotinib detaches from the loop, and in the last step (195-500 ps) it moves away from the protein and enters the solvent region (Fig. 3.B). Differently, for Imatinib it is not possible to detect a clear maximum, and the force tend not to variate during the simulation. This lower rupture force for Imatinib (about 200 kJ/mol/nm less than Nilotinib) reflects the easier unbinding of Imatinib from RBD, in line with our data showing a lower binding affinity.

Discussion

SARS-CoV-2 invades human cells via ACE2, a transmembrane protein expressed on the surface of alveolar cells of the lungs. Upon binding of ACE2, viral and host cell membranes fuse and the virus enters into the host cell. This results in the development of an infectious disease, called COVID-19, which is associated with a major immune inflammatory response. Deaths are caused by respiratory failure, which have been linked to a cytokine storm with high serum levels of pro-inflammatory cytokines and chemokines [18]. There are currently no approved vaccines or drugs that specifically target Coronavirus infection, and, despite several ongoing clinical trials, treatment options have been based on different clinical approaches with limited background testing. An exponentially growing number of computational studies have tried to provide molecular data in support of these novel potential COVID-19 treatments [19 20 21 16].

The aim of this proof of principle study was to propose a robust *in silico* protocol that overcame limitations of classic virtual screening studies [22]. The role of hydration patterns in target recognition and binding is completely absent in docking simulations. Furthermore, in most virtual screenings, while the ligand is flexible, proteins are only semi-flexible, which affects both the resulting pose of the ligand and the scoring system [23]. More reliable information can only be obtained by MD simulations, which, despite being computationally expensive, allow to take into account macromolecules unique features, such as conformational flexibility, charge distribution, and hydration patterns in target recognition, drug binding, and drug unbinding [24 25]. In this study we

coupled docking with MD, SuMD and SMD to identify a Spike protein – ACE2 interaction inhibitor. Transmission electron microscope image of SARS-CoV-2 have shown how the viral envelope is densely populated by the S protein, which, due to its role in pathogenesis, is the main target of neutralizing antibodies and vaccines [26]. An analysis of the crystal structure of the RBD with ACE2, reveals that the RBD of the S protein has a relatively flat surface, which would be unsuitable for drug targeting. Previous studies have shown that the analysis of protein dynamics allows for the identification of transient pockets where small molecules can bind proteins [27]. We identified a transient pocket with druggability features on the RBD which may represent a hot spot (Venditti et al., 2007). Indeed, comparison with the structure of SARS-CoV S protein in complex with a neutralising antibody isolated from a SARS-CoV survivor shows that the pocket we identified lies on the same surface recognised by the CDRs of the antibody (Walls et al., 2019). We retrieved the structure of the protein with an open pocket from the trajectory of the MD simulation and we used it for a virtual screening of 1223 FDA-approved drugs. The advantage of focusing on FDA-approved drugs is that the safety issues are all within suitable bounds and are well understood, meaning that they could proceed to clinical trial reasonably quickly. The compounds showing the higher binding energy were Nilotinib and Imatinib. Imatinib is the first-generation drug targeted against chronic myelogenous leukaemia, while Nilotinib was a second-generation, aimed to overcome some of the resistance mechanisms acquired following Abl kinase mutations [17]. The two drugs were also selected for their reported minimal side effects and specificity for Abl, Kit, and PDGFR kinases, suggesting lack of binding to other human proteins (Cole et al., 2020). The two drugs share a similar structure and bind on the same surface on the RBD. While they both are potentially viable PPI inhibitors, they do not share similar binding modes. In fact, we noticed that Imatinib sample a larger space on the binding pocket than Nilotinib during the MD simulations. Liu & Kokubo [28] have used MD simulations to identify more biologically representative binding poses of ligands and have shown that large changes of poses during MD simulations are linked to a poor binding stability of the ligands. This is in agreement with our SMD results, which elegantly showed that Imatinib is not tightly bound to the protein and escapes the binding site easily, differently from Nilotinib for which we were able to see an unbinding event and an exit rout from the binding pocket. Interestingly, we also noticed that the moment of inertia (MOI) of RBD bound to Nilotinib is higher than the MOI of RBD alone or in complex with Imatinib (Fig. S3.D). An increase in MOI has been associated with a loss of cross correlations, which could be linked to a reduced protein structural stability [29]. Although beyond the aim of this study, we speculate that Nilotinib may have a secondary PPI inhibition mechanism by affecting the Spike protein stability.

While writing this paper, several drug repurposing studies targeting the S protein have been published. Interestingly, Smith and Smith [19] and Senathilake et al. [21] carried out a virtual screening on the same surface we identified as a transient pocket. Binding energies of the proposed compounds are however one order of magnitude lower than the one we observed for Nilotinib. This

is very likely linked to the protein structures used for virtual screening and/or a binding pocket not being in the optimal open conformation, highlighting the strength of our *in silico* approach.

Our results show the importance of taking into account the full structural features of a protein-ligand complex and how a combination of MD simulations may help predict the validity of a proposed inhibitor. Our work suggests that Nilotinib could be a potential initial compound able to prevent SARS-CoV-2 infection.

Methods

Structural Resources

3D Structure and FASTA sequence of SARS-CoV-2 RBD in complex with human hACE2 (PDB ID 6VW1) were retrieved from the RCSB Protein Data Bank [30] . To avoid errors during the molecular dynamic (MD) simulations, missing side chains and steric clashes in PDB files were adjusted by homology modelling, using PyMOD2.0 and MODELLER v.9.3 [31]. 3D structures were validated using PROCHECK [32]. GROMACS 2019.3 [33] with AMBER99SB-ILDN force field was used to resolve high energy intramolecular interaction before docking simulations. Structures were immersed in a cubic box filled with TIP3P water molecules and counter ions to balance the net charge of the system. Simulations were run applying periodic boundary conditions. The energy of the system was minimized with 5.000 steps of minimization with the steepest descent algorithm and found to converge to a minimum energy with forces less than 100 kJ/mol/nm. A short 10 ns classic Molecular Dynamics (cMD) was performed to relax the system.

All the cMD simulations were performed integrating each time step of 2 fs; a V-rescale thermostat maintained the temperature at 310 K and Berendsen barostat maintained the system pressure at 1 atm, with a low dumping of 1 ps^{-1}; the LINCS algorithm constrained the bond lengths involving hydrogen atoms.

Transient pockets and virtual screening

A 100 ns cMD simulations was used, as described above, for the identification of transient pockets. Transient pockets were identified by analysing MD trajectories of of SARS-CoV-2 RBD structure with EPOS tool [34], using parameters by default [35]. The volumes of the transient pockets during the simulation were measured using POVME [36]. Open pockets in close proximity to ACE2 binding site were selected based on the depth and polarity of the cavity. A box with dimensions of 25, 25, and 21 Å was created around the transient pocket using Autodock Tools [37]. Subsequently, a virtual screening of 1223 FDA-approved drugs obtained from Drugbank [38] was carried out on SARS-CoV-

2 RBD using AutoDock/VinaXB [39]. MGLTOOLS scripts [37] and OpenBabel [40] were used respectively to convert protein and ligand files and added gasteiger partial charges.

Supervised Molecular Dynamics (SuMD) simulations

SuMD were used to sample the binding of hACE2 to RBD, as well as to probe the binding of hACE2 to RBD-Nilotinib/Imatinib complexes. SuMD methodology relies on a tabu-like algorithm that monitors the distance between hACE2 and centre of mass of the RBD binding site during unbiased MD simulations to sample a binding event in the range of nanoseconds [41]. The protocol is based on performing a series of short unbiased MD simulations, where after each simulation the distance points collected at regular time intervals are fitted into a linear function. If the resulting slope is negative, then hACE2 is getting closer to the RBD binding site and the MD steps are kept, if it the slope is not negative, then the simulation is restarted by randomly assigning the atomic velocities. We used an SuMD step of 1000 ps, with a constant temperature and pressure of 310 K and 1 atm respectively. When the distance between the hACE2 and RBD reached 5 Å or less, then the supervision was disabled, and a 10 ns cMD simulation was performed. The analysis was performed with an in-house written python and bash script.

Steered Molecular Dynamics (SMD) simulations

In order to evaluate the binding interaction between RBD and Nilotinib or Imatinib, the RBD-Nilotinib/Imatinib complexes were simulated to dissociate using a 500 ps SMD simulation by Constant Force Pulling of 250 KJ/mol/nm. While the backbone of RBD was not allowed to move, Nilotinib and Imatinib experienced a constant force in x, y, z direction, specifically (0, 250, 0) for both compounds. Nilotinib and Imatinib were pulled with an external force in the NPT ensemble at 1 atm and 310 K with 2 fs time steps. MD analyses was performed with GROMACS 2019.3 package and displayed with GRACE.

Molecular mechanics/Poisson-Boltzmann surface area (MM/PBSA)

MM/PBSA is a standard method used to estimate the binding free energy of a protein-ligand complex. The last 10 ns of the cMD trajectory for both Nilotinib and Imatinib in complex with RBD were extracted for MM/PBSA calculations [42]. The binding energy were calculated using the g_mmpbsa package within GROMACS [43]. In short, the binding energy are defined as:

$$\Delta G_{Binding} = G_{Complex} - (G_{Protein} + G_{Ligand})$$

where, $G_{Complex}$, $G_{Protein}$ and G_{Ligand} are respectively the total free energy of the protein-ligand complex, of RBD and Nilotinib or Imatinib.

References

1. Andersen, K. G., Rambaut, A., Lipkin, W. I., Holmes, E. C. & Garry, R. F. The proximal origin of SARS-CoV-2. *Nat. Med.* (2020) doi:10.1038/s41591-020-0820-9.
2. Bernini, A. *et al.* Prediction of quaternary assembly of SARS coronavirus peplomer. *Biochem. Biophys. Res. Commun.* (2004) doi:10.1016/j.bbrc.2004.10.156.
3. Lai, C. C., Shih, T. P., Ko, W. C., Tang, H. J. & Hsueh, P. R. Severe acute respiratory syndrome coronavirus 2 (SARS-CoV-2) and coronavirus disease-2019 (COVID-19): The epidemic and the challenges. *International Journal of Antimicrobial Agents* (2020) doi:10.1016/j.ijantimicag.2020.105924.
4. Bernini, A. *et al.* Tertiary structure prediction of SARS coronavirus helicase. *Biochem. Biophys. Res. Commun.* (2006) doi:10.1016/j.bbrc.2006.03.069.
5. Shang, W., Yang, Y., Rao, Y. & Rao, X. The outbreak of SARS-CoV-2 pneumonia calls for viral vaccines. *npj Vaccines* (2020) doi:10.1038/s41541-020-0170-0.
6. Walls, A. C. *et al.* Structure, Function, and Antigenicity of the SARS-CoV-2 Spike Glycoprotein. *Cell* (2020) doi:10.1016/j.cell.2020.02.058.
7. Li, F., Li, W., Farzan, M. & Harrison, S. C. Structural biology: Structure of SARS coronavirus spike receptor-binding domain complexed with receptor. *Science (80-.).* (2005) doi:10.1126/science.1116480.
8. Yan, R. *et al.* Structural basis for the recognition of SARS-CoV-2 by full-length human ACE2. *Science (80-.).* (2020) doi:10.1126/science.abb2762.
9. Hoffmann, M. *et al.* SARS-CoV-2 Cell Entry Depends on ACE2 and TMPRSS2 and Is Blocked by a Clinically Proven Protease Inhibitor. *Cell* (2020) doi:10.1016/j.cell.2020.02.052.
10. Li, F. Structure, Function, and Evolution of Coronavirus Spike Proteins. *Annu. Rev. Virol.* (2016) doi:10.1146/annurev-virology-110615-042301.
11. Ou, X. *et al.* Characterization of spike glycoprotein of SARS-CoV-2 on virus entry and its immune cross-reactivity with SARS-CoV. *Nat. Commun.* (2020) doi:10.1038/s41467-020-15562-9.
12. Wrapp, D. *et al.* Cryo-EM structure of the 2019-nCoV spike in the prefusion conformation. *Science (80-.).* (2020) doi:10.1126/science.aax0902.
13. Zheng, B. J. *et al.* Synthetic peptides outside the spike protein heptad repeat regions as potent inhibitors of SARS-associated coronavirus. *Antivir. Ther.* (2005).
14. Zhu, Z. *et al.* Potent cross-reactive neutralization of SARS coronavirus isolates by human monoclonal antibodies. *Proc. Natl. Acad. Sci. U. S. A.* (2007)

doi:10.1073/pnas.0701000104.

15. Sui, J. *et al.* Potent neutralization of severe acute respiratory syndrome (SARS) coronavirus by a human mAb to S1 protein that blocks receptor association. *Proc. Natl. Acad. Sci. U. S. A.* (2004) doi:10.1073/pnas.0307140101.
16. Zhou, Y. *et al.* Network-based drug repurposing for novel coronavirus 2019-nCoV/SARS-CoV-2. *Cell Discov.* (2020) doi:10.1038/s41421-020-0153-3.
17. Cole, A. L. *et al.* Comparative Safety and Health Care Expenditures Among Patients With Chronic Myeloid Leukemia Initiating First-Line Imatinib, Dasatinib, or Nilotinib. *JCO Oncol. Pract.* (2020) doi:10.1200/jop.19.00301.
18. Feldmann, M. *et al.* Trials of anti-tumour necrosis factor therapy for COVID-19 are urgently needed. *Lancet* (2020) doi:10.1016/S0140-6736(20)30858-8.
19. Smith, M. & Smith, J. C. Repurposing Therapeutics for COVID-19: Supercomputer-Based Docking to the SARS-CoV-2 Viral Spike Protein and Viral Spike Protein-Human ACE2 Interface. *ChemRxiv* (2020) doi:10.26434/chemrxiv.11871402.v3.
20. Wu, C. *et al.* Analysis of therapeutic targets for SARS-CoV-2 and discovery of potential drugs by computational methods. *Acta Pharm. Sin. B* (2020) doi:10.1016/j.apsb.2020.02.008.
21. Senathilake, K., Samarakoon, S. & Tennekoon, K. Virtual Screening of Inhibitors Against Spike Glycoprotein of 2019 Novel Corona Virus: A Drug Repurposing Approach. (2020) doi:10.20944/PREPRINTS202003.0042.V1.
22. Lavecchia, A. & Giovanni, C. Virtual Screening Strategies in Drug Discovery: A Critical Review. *Curr. Med. Chem.* (2013) doi:10.2174/09298673113209990001.
23. Hutter, M. C. The current limits in virtual screening and property prediction. *Future Medicinal Chemistry* (2018) doi:10.4155/fmc-2017-0303.
24. Saravanan, K., Kalaiarasi, C. & Kumaradhas, P. Understanding the conformational flexibility and electrostatic properties of curcumin in the active site of rhAChE via molecular docking, molecular dynamics, and charge density analysis. *J. Biomol. Struct. Dyn.* (2017) doi:10.1080/07391102.2016.1264891.
25. Venditti, V. *et al.* MD and NMR studies of α-bungarotoxin surface accessibility. *Biochem. Biophys. Res. Commun.* (2007) doi:10.1016/j.bbrc.2007.02.094.
26. Walls, A. C. *et al.* Unexpected Receptor Functional Mimicry Elucidates Activation of Coronavirus Fusion. *Cell* (2019) doi:10.1016/j.cell.2018.12.028.
27. Eyrisch, S. & Helms, V. What induces pocket openings on protein surface patches involved in protein - Protein interactions? *J. Comput. Aided. Mol. Des.* (2009) doi:10.1007/s10822-008-9239-y.
28. Liu, K. & Kokubo, H. Exploring the Stability of Ligand Binding Modes to Proteins by Molecular Dynamics Simulations: A Cross-docking Study. *J. Chem. Inf. Model.* (2017)

doi:10.1021/acs.jcim.7b00412.

29. Zhou, Y., Cook, M. & Karplus, M. Protein motions at zero-total angular momentum: The importance of long-range correlations. *Biophys. J.* (2000) doi:10.1016/S0006-3495(00)76527-1.

30. Shang, J. *et al.* Structural basis of receptor recognition by SARS-CoV-2. *Nature* (2020) doi:10.1038/s41586-020-2179-y.

31. Janson, G., Zhang, C., Prado, M. G. & Paiardini, A. PyMod 2.0: improvements in protein sequence-structure analysis and homology modeling within PyMOL. *Bioinformatics* (2017) doi:10.1093/bioinformatics/btw638.

32. Laskowski, R. A., MacArthur, M. W., Moss, D. S. & Thornton, J. M. PROCHECK: a program to check the stereochemical quality of protein structures. *J. Appl. Crystallogr.* (1993) doi:10.1107/s0021889892009944.

33. Berendsen, H. J. C., van der Spoel, D. & van Drunen, R. GROMACS: A message-passing parallel molecular dynamics implementation. *Comput. Phys. Commun.* (1995) doi:10.1016/0010-4655(95)00042-E.

34. Brady, G. P. & Stouten, P. F. W. Fast prediction and visualization of protein binding pockets with PASS ps:surface,sasa,cavity,software,hole,channel,tunnel,. *J. Comput. Aided. Mol. Des.* (2000).

35. Bernini, A. *et al.* Toward a generalized computational workflow for exploiting transient pockets as new targets for small molecule stabilizers: Application to the homogentisate 1,2-dioxygenase mutants at the base of rare disease Alkaptonuria. *Comput. Biol. Chem.* (2017) doi:10.1016/j.compbiolchem.2017.08.008.

36. Wagner, J. R. *et al.* POVME 3.0: Software for Mapping Binding Pocket Flexibility. *J. Chem. Theory Comput.* (2017) doi:10.1021/acs.jctc.7b00500.

37. Morris, G. M. *et al.* Software news and updates AutoDock4 and AutoDockTools4: Automated docking with selective receptor flexibility. *J. Comput. Chem.* (2009) doi:10.1002/jcc.21256.

38. Wishart, D. S. *et al.* DrugBank 5.0: A major update to the DrugBank database for 2018. *Nucleic Acids Res.* (2018) doi:10.1093/nar/gkx1037.

39. Koebel, M. R., Schmadeke, G., Posner, R. G. & Sirimulla, S. AutoDock VinaXB: Implementation of XBSF, new empirical halogen bond scoring function, into AutoDock Vina. *J. Cheminform.* (2016) doi:10.1186/s13321-016-0139-1.

40. O'Boyle, N. M. *et al.* Open Babel: An Open chemical toolbox. *J. Cheminform.* (2011) doi:10.1186/1758-2946-3-33.

41. Sabbadin, D., Salmaso, V., Sturlese, M. & Moro, S. Supervised molecular dynamics (SuMD) approaches in drug design. in *Methods in Molecular Biology* (2018). doi:10.1007/978-1-4939-8630-9_17.

42. Homeyer, N. & Gohlke, H. Free energy calculations by the Molecular Mechanics Poisson-Boltzmann Surface Area method. *Mol. Inform.* (2012) doi:10.1002/minf.201100135.
43. Kumari, R., Kumar, R. & Lynn, A. G-mmpbsa -A GROMACS tool for high-throughput MM-PBSA calculations. *J. Chem. Inf. Model.* (2014) doi:10.1021/ci500020m.

Figure 1. (A) Surface representation of the structure of the RBD of the S protein having an open pocket conformation. The transient pocket surface patch is depicted in brown. In the zoomed region it is possible to see a detailed structural representation of the open pocket conformation. Residues laying on the pocket surface have been labelled and are shown in stick. (B-C) Structural representations of the (B) RBD-Nilotinib and (C) RBD-Imatinib complexes resulting from docking simulations. Residues forming direct interactions with the drugs are shown as brown sticks. Hydrogen bonds are indicated with green dashed lines and the halogen bond is shown with red dashed lines.

Figure 2. (A) MM/PBSA binding energy against simulation time for Nilotinib (dotted line) and Imatinib (dashed line). (B) Per residue energy of interaction with Nilotinib (dotted line) and Imatinib (dashed line). Energy of interaction during the MM/PBSA calculations is shown against the RBD residues numbers.

Figure 3. (A) Force profiles of drugs pulled out of the RDB transient pocket along the unbinding pathway, Nilotinib (dotted line) and Imatinib (dashed line). (B) Structural representations showing position of Nilotinib (blue ball-and-stick) and Imatinib (red ball-and-stick) on RBD (white cartoon) during the different stages of the unbinding process.

Author contributions

Alfonso Trezza conceived the original idea of the work and was in charge of overall direction and planning. He acquired, analysed and interpreted of data and reviewed the manuscript.
Daniele Iovinelli created new algorithms used in the work.
Filippo Prischi made substantial contributions to the design of the work and He drafted the manuscript.
Annalisa Santucci and Ottavia Spiga reviewed the paper and provided positive opinion for this work.
All authors approved the submitted version.

Corresponding author

Filippo Prischi and Ottavia Spiga

Competing interests

The authors declare no competing interests.

Referee suggestions

Vincenzo Venditti, Assistant Professor at the Department of Chemistry of Iowa State University, USA.
Contact: venditti@iastate.edu

Alfonso De Simone, Reader in Structural Biology at the Faculty of Natural Sciences, Department of Life Sciences, Imperial College, London, UK
Contact: a.de-simon@imperial.ac.uk

Franca Fraternali, Professor of Bioinformatics and Computational Biology, King's College London, UK
Contact: franca.fraternali@kcl.ac.uk

Miquel Adrover, Departament de Química, Universitat de les Illes Balears Institut, Universitari d'Investigació en Ciències de la Salut (IUNICS), Institut de Recerca en Ciències de la Salut (IdISBa), Palma de Mallorca, Spain.
Contact: miquel.adrover@uib.es

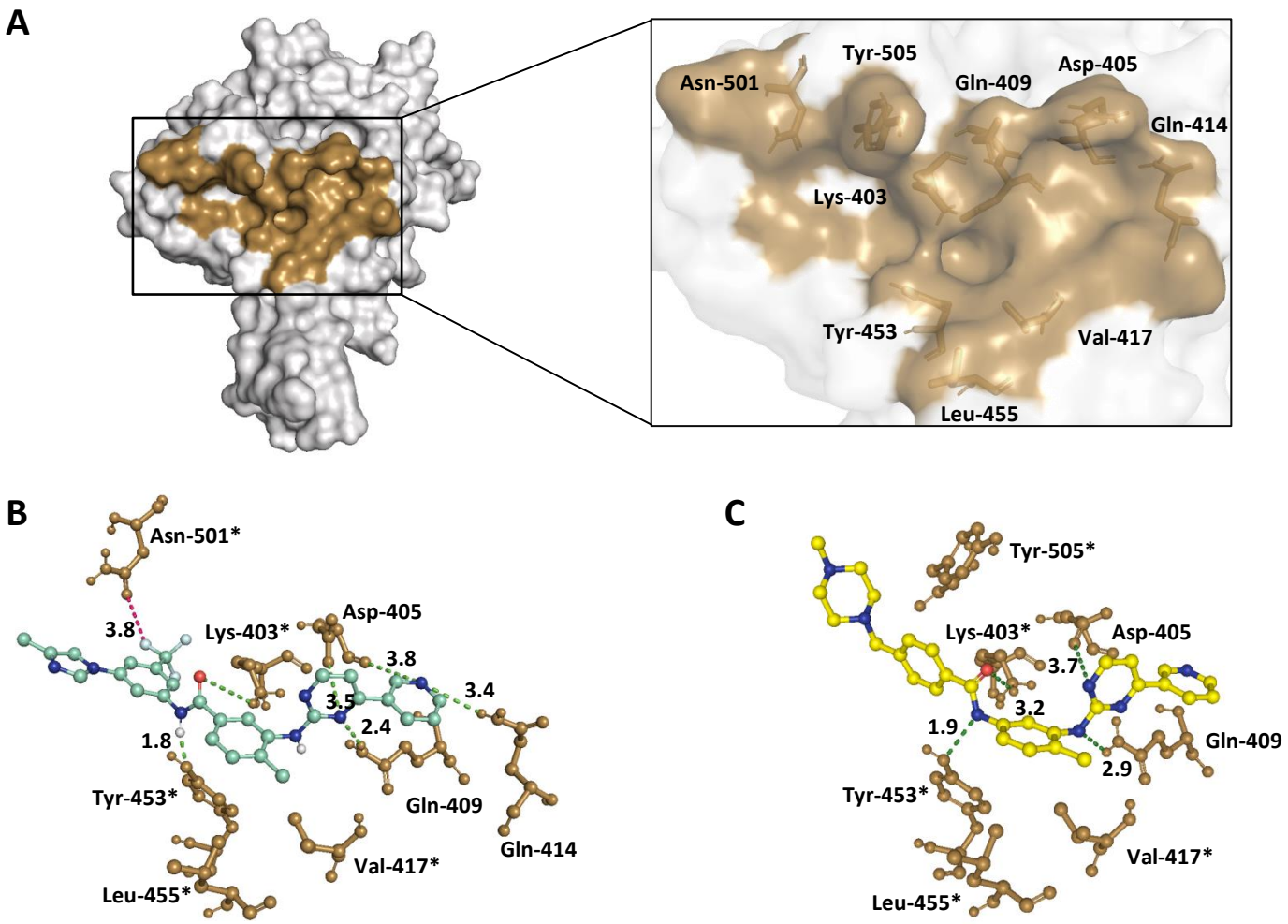

Figure 1.

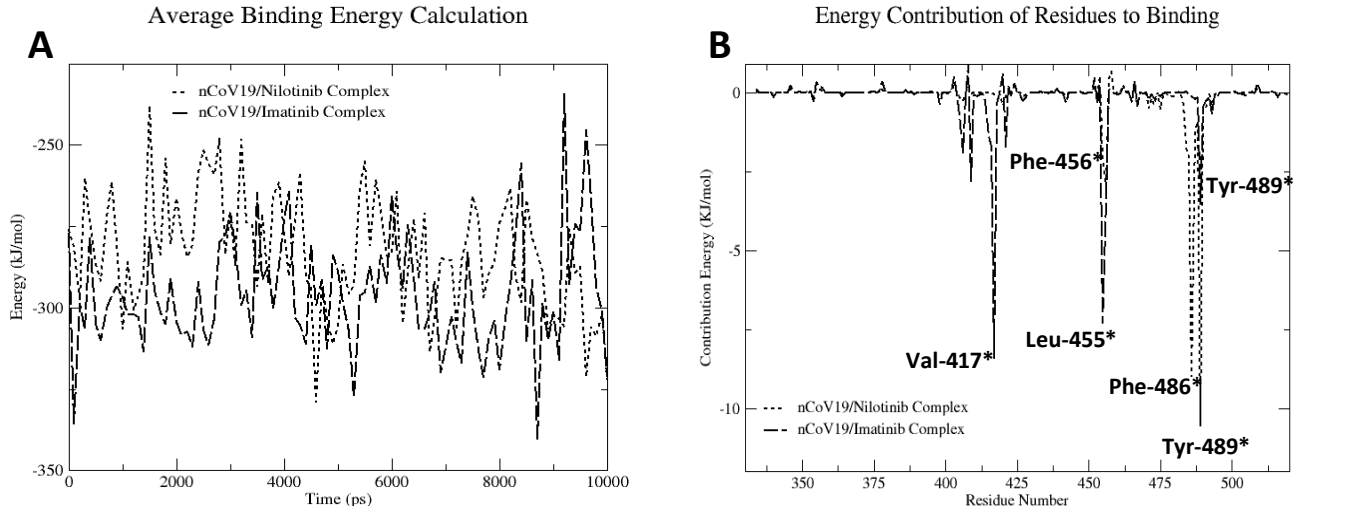

Figure 2.

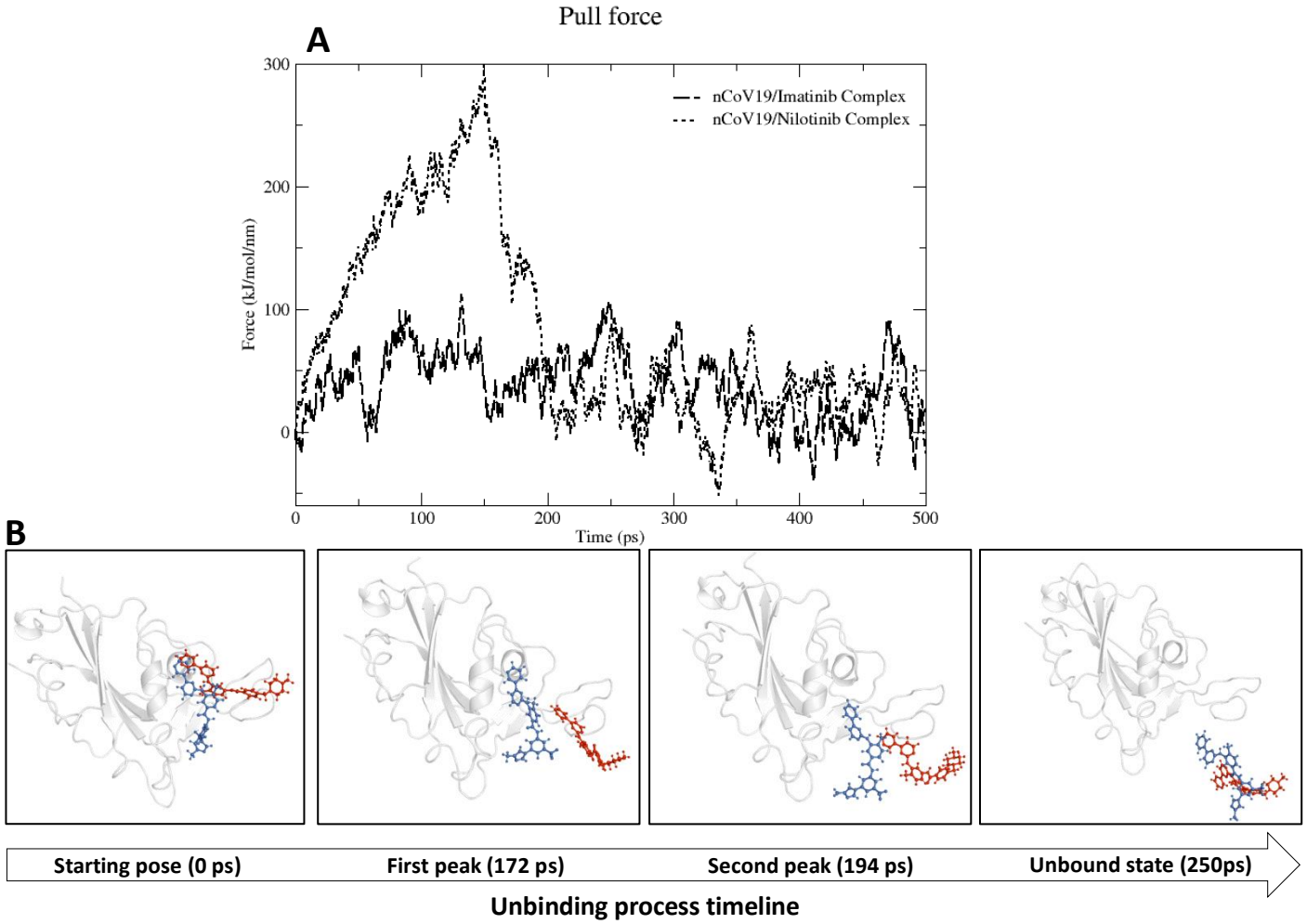
A
Pull force
nCoV19/Imatinib Complex
nCoV19/Nilotinib Complex
Force (kJ/mol/nm)
Time (ps)
0
100
200
300
400
500
B
Starting pose (0 ps)
First peak (172 ps)
Second peak (194 ps)
Unbound state (250ps)
Unbinding process timeline

Figure 3.